

# Pattern Selection and the Direction of Stripes in Two-Dimensional Turing Systems for Skin Pattern Formation of Fishes

Hiroto SHOJI\* and Yoh IWASA

*Department of Biology, Faculty of Sciences, Kyushu University, Fukuoka 812-8581, Japan*

*\*E-mail address: shoji@bio-math10.biology.kyushu-u.ac.jp*

(Received November 29, 2002; Accepted December 25, 2002)

**Keywords:** Reaction-Diffusion System, Turing, Pattern Selection, Anisotropic Diffusion, Directionality of Stripes

**Abstract.** Turing mechanism explains the pattern formation in a uniform field in which two substances (e.g. activator and inhibitor) interact locally and diffuse randomly. Two-dimensional Turing models can generate stationary spatial patterns either with stripes or with spots, and have been adopted to explain the skin pattern formation of animals. We first discuss the effect of the choice of reaction terms on pattern selection, whether spots or stripes are formed. It is shown that the relative distance of the equilibrium level of activator between the upper and lower limitations has a very strong effect on the pattern selection. Secondly, we focus on the direction of the stripes generated by Turing model with anisotropic diffusion in order to explain the directionality of stripes on fish skin in closely related species. Relative magnitude of anisotropy of the two substances is shown to determine whether stripes are vertical or horizontal.

## 1. Introduction

Some animals have striped pattern on their skin, exemplified by zebra or tiger's coating. The developmental pattern formation of animal coating has been studied mathematically by Turing system (MEINHARDT, 1982; MURRAY, 1989). It is a pair of partial differential equations, and represents the time development of reacting and diffusing chemicals, which can evolve spontaneously to spatially heterogeneous stationary pattern from an initially uniform distribution (TURING, 1952). TURING (1952) specifically considered a system of two chemicals, an activator and an inhibitor, where the activator enhances its own production rate and also promotes the production of the inhibitor whilst the inhibitor suppresses both activator and inhibitor. The diffusion coefficient of the inhibitor is much larger than that of the activator. Without diffusion, the local reaction of the two substances is stable and converges to the equilibrium. However, with diffusion, the uniform distributions of both substances with concentrations at the equilibrium are unstable, and a spatially heterogeneous pattern emerges spontaneously, called Turing instability. This simple mechanism suggests that reaction of a small number of chemicals and their random diffusion can create stable non-uniform patterns in a perfectly homogeneous field.

MEINHARDT (1982) discussed many cases of pattern formation in development that are likely to be explained by reaction-diffusion model, including regeneration and pattern formation of hydras (MEINHARDT, 1982). MURRAY (1989) also explained various phenomena of biological pattern formation including the patterns of animal coating. Although patterns of mammal coating are quite suggestive of the involvement of Turing mechanism, their pattern is formed in early developmental stages, and the number of stripes does not change in their lifetime even if the body size grows considerably. In contrast, the stripe pattern on fish skin changes as the fish body size increases (KONDO and ASAI, 1995). The number of stripes increases with the body size but the width of each stripe and their distance between stripes remain almost unchanged. KONDO and ASAI (1995) studied the skin patterns of several species of tropical fishes, and showed that the change of their skin patterns can be explained very accurately by a simple reaction-diffusion model of Turing type.

Motivated by these past studies, we discuss two new problems in the Turing system. First, we study the mechanism of pattern selection. A Turing system on a two-dimensional plane gives either striped pattern or spotted pattern for values of parameters, which cause Turing instability in an one-dimensional system (Fig. 1). There are three major classes of the spatial patterns. Figures 1a and 1b illustrate a “spot pattern” and a “stripe pattern”, respectively, for the location with high activator density. Figure 1c illustrates a “reversed spot pattern”, in which areas with a low activator density (dark) exist in patches that scatter over the plane, whereas the areas with a high activator density (white) are connected. There is an interesting problem, here, how the choice of the reaction terms in Turing modes affects the tendency to generate either stripes, or spots, or reversed spots.

Different pigment patterns of animal coating presumably serve as cryptic coloration or social signals in group forming species. Comparative study of cichlid fishes with stripes shows a significant correlation between social structure of the species and the direction of stripes, suggesting their role in social interaction (SEEHAUSEN *et al.*, 1999). Many species in fishes have pigment patterns similar to surrounding circumstances, to achieve cryptic coloration, exemplified by a goby in genus *Gobiidae* and a flounder *Paralichthys olivaceus*,

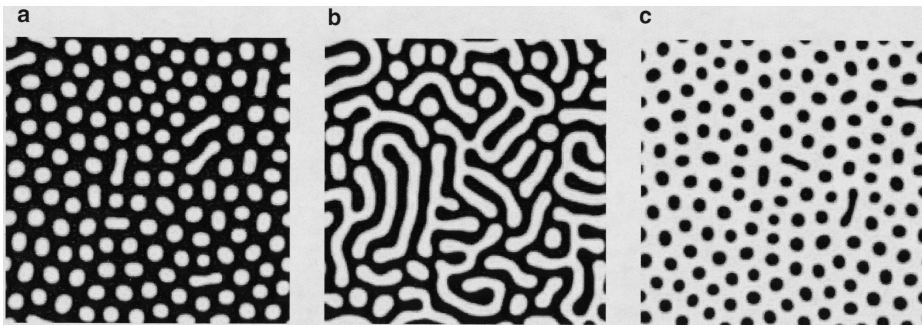


Fig. 1. Spatial patterns generated by a two-dimensional Turing model expressed by Eqs. (1), (4) and (5). The white color indicates the area with a higher activator density  $u$ . Parameters are the same except  $u_{\text{upper}}$ : (a) spot pattern ( $u_{\text{upper}} = 50.0$ ), (b) stripe pattern ( $u_{\text{upper}} = 10.00$ ), (c) reversed spot pattern ( $u_{\text{upper}} = 4.10$ ). Other parameters are:  $A = 0.90$ ,  $B = 1.20$ ,  $C = 0.20$ ,  $d = 20.0$ ,  $\gamma = 10000$  and  $u_{\text{lower}} = 0.0$ .

suggesting that the pattern might serve as a means of predator avoidance (KUWAMURA and KARINO, 1999). Within the same species of fish *Hypostomus plecostomus*, some subspecies has spot pattern and others has stripes (YAMAGUCHI, 2002).

Secondly, the directionality of stripes formed in Turing systems provides an interesting problem. Since fish have scales, fish skin is morphologically different along the AP axis and along the dorso-ventral (DV) axis. Therefore it is plausible to assume that the diffusion coefficient is different between directions. We study the reaction-diffusion model where the substances can diffuse faster in a certain specific direction than in a direction perpendicular to it. Hence the diffusion of the two substances can be anisotropic. Results of numerical analysis in this work explain many features of pattern formation shown by several species in genus *Genicanthus*.

We also develop a heuristic argument of the direction of stripes in more general situations in which the diffusive direction may differ between the two substances. As a result we have derived a formula for the direction of stripes, based on the most unstable mode of deviation from the uniform steady state.

## 2. Turing System

TURING (1952) showed that two diffusive chemicals that react each other can generate spatially heterogeneous patterns spontaneously from a uniform initial distribution. In general, the model can be written as follows,

$$\frac{\partial u}{\partial t} = \nabla^2 u + \mathcal{F}(u, v), \quad \text{and} \quad \frac{\partial v}{\partial t} = d\nabla^2 v + \mathcal{G}(u, v), \quad (1)$$

where  $u$  and  $v$  are the concentrations of two substances which differ in diffusivity. By rescaling the space variable, we made the diffusion coefficient of  $u$  equal to 1. On the other hand, two reaction terms are multiplied by a common factor  $\gamma$ , and the diffusion coefficient for  $v$  is replaced by the ratio of diffusion coefficient of the two substances, denoted by  $d$ . Here we assume that  $d$  is larger than 1, and hence diffusivity of  $v$  is larger than that of  $u$ .

Now we consider the equilibrium  $(u_0, v_0)$  of ordinary differential equations corresponding to partial differential Eq. (1). It satisfies:  $f(u_0, v_0) = 0$ , and  $g(u_0, v_0) = 0$ . This is linearly stable in the ordinary differential equation:

$$\frac{\partial f}{\partial u} + \frac{\partial g}{\partial v} < 0, \quad \text{and} \quad \frac{\partial f}{\partial u} \frac{\partial g}{\partial v} - \frac{\partial f}{\partial v} \frac{\partial g}{\partial u} > 0, \quad (2)$$

where all the partial derivatives are evaluated at equilibrium  $(u_0, v_0)$ . Second, we consider the local stability of the uniform steady state  $u = u_0$  and  $v = v_0$ . This steady state solution is unstable in the partial differential equations given by Eq. (1). This leads to:

$$d \frac{\partial f}{\partial u} + \frac{\partial g}{\partial v} > 0, \quad \text{and} \quad \left( d \frac{\partial f}{\partial u} + \frac{\partial g}{\partial v} \right)^2 - 4d \left( \frac{\partial f}{\partial u} \frac{\partial g}{\partial v} - \frac{\partial f}{\partial v} \frac{\partial g}{\partial u} \right) > 0. \quad (3)$$

The model satisfying Eqs. (2) and (3) is called a Turing system, and the parameter region for a given model to be a Turing system is called Turing space (MURRAY, 1989).

SHOJI *et al.* (2003b) examined the dimensionless reaction diffusion system as Eq. (1) with the linear reaction terms (following KONDO and ASAI, 1995; ASAI *et al.*, 1999):

$$f(u, v) = Au - v + C, \quad \text{and} \quad g(u, v) = Bu - v - 1, \quad (4)$$

where  $A$ ,  $B$  and  $C$  are constants.

In the numerical calculation of Eqs. (1) and (4), the deviation of two variables from the equilibrium increases with time and diverges to positive and negative infinity. For the model to have a stable stationary distribution of finite magnitude, we need to add terms to constrain the variables within a finite range.

### 3. Pattern Selection Problem—Spot, Stripe, or Reversed Spot

We studied how the choice of the reaction terms in Turing modes affects the tendency to generate either stripes, or spots, or reversed spots. We focus on the role of non-linearity in reaction terms that constrain the variables within a fixed range.

#### 3.1. Periodic pattern in one dimensional

Before examining the pattern selection of two-dimensional models, we first consider the condition in which stable periodic pattern can be formed in a one-dimensional Turing model with linear reaction terms and constraints. We can show that linear models can generate stable periodic patterns if both variables are constrained from above and from below (e.g. KONDO and ASAI, 1995). To be specific, we introduced the constraint of  $u$ , as follows:

$$u_{\text{lower}} \leq u \leq u_{\text{upper}}, \quad (5)$$

where  $u_{\text{lower}}$  and  $u_{\text{upper}}$  are constants. We call these as lower and upper limitations, respectively. We may also introduce a similar constraint with respect to  $v$ . There are four possible ways of constraint: the upper limitation of  $u$ , the lower limitation of  $u$ ; the lower upper limitation of  $v$ ; and the lower limitation of  $v$ . We studied all the possible combinations of these four ways of introducing constraints. The result is very clear—the activator, but not the inhibitor, must be constrained both from above and from below for the model to generate a stable periodic pattern in one-dimensional model, given by Eqs. (1) and (4), provided that parameters are within the Turing space. See SHOJI *et al.* (2003b) for detail.

#### 3.2. Stripe, spots and reversed spots generated by linear system

We then discuss two-dimensional patterns generated by linear model given by Eqs. (1) and (4) with constraint Eq. (5). We have done all the simulation in this chapter by the same analysis explained below. We chose parameter and parameter range of reaction term as:  $\gamma = 10000$ ,  $d = 20.0$ ,  $C = 0.20$ ,  $0.0 \leq A \leq 1.2$  and  $0.0 \leq B \leq 6.0$ . Most of these parameters are in the Turing Space (see Fig. 2). The simulations were performed with periodic boundary

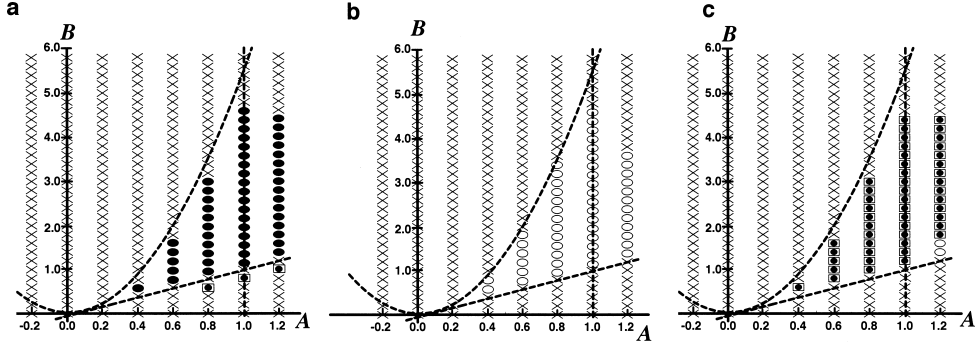


Fig. 2. The parameter regions in which stripes, spots, and reversed spots were generated. Dynamics expressed by Eqs. (1) and (4) were adopted. The upper and lower limitations were realized by resetting the variables whenever they go outside of the allowed interval. ● with box: reversed spot, ○: stripe pattern, ●: spot pattern, ×: homogeneous pattern. The area surrounded by four broken lines is the Turing space derived from Eqs. (2) and (3). Other parameters are fixed as:  $C = 0.20$ ,  $d = 20.0$  and  $\gamma = 10000$ . (a) The distance from the equilibrium point to the upper limitation is 5.0 and one to lower limitation is 1.0. Spots pattern are produced in most of the Turing space. (b) The distance from the equilibrium point to upper limitation and the one to the lower limitation are both 1.0. The stripe patterns were produced in most of the Turing space. (c) The distance from the equilibrium point to upper limitation is 1.0 and one to lower limitation is 5.0. The reversed spots pattern were produced in the large part of the Turing space.

condition in a square domain of size:  $2.0 \times 2.0$  (grid:  $200 \times 200$ ). A simple explicit scheme is adopted. To satisfy the stability condition for numerical analysis, mesh size was chosen to be  $1.0 \times 10^{-6}$ . The fixed parameter was  $\gamma = 10000$ . We tested three initial conditions where value of  $u$  and  $v$  are equilibrium values added by small random deviations. The time at which we stopped calculation was sufficiently long, and we can safely regard that the pattern would no longer change from the one obtained in the end of simulation even if we increase the calculation time further.

We examine the effect of the constraint in determining pattern selection in the two-dimensional model. First, we note that, because of linear kinetics adopted here, the property of the model should not be changed by rescaling variables and time or space parameters. Hence whether the model generates patterns with spots, stripes or reversed spots should be unchanged if  $|u_{\max} - u_{\text{eq}}|$  and  $|u_{\text{eq}} - u_{\min}|$  are multiplied by the same factor, and hence only the ratio of  $|u_{\max} - u_{\text{eq}}|$  to  $|u_{\text{eq}} - u_{\min}|$  affects the pattern selection. We here focus on the patterns generated by each parameter of Eqs. (1) and (4) with constraint Eq. (5). Due to the linear nature of the kinetics, shifting of variables also should not affect the pattern selection, indicating that the results is independent of parameter  $C$  in Eq. (4).

In Fig. 2, we have different cases of the ratio of  $|u_{\max} - u_{\text{eq}}|$  and  $|u_{\text{eq}} - u_{\min}|$ . Different symbols indicate the produced patterns. We judged each pattern to be one of the three by eye. Two axes are  $A$  and  $B$ . Figure 2a shows the results when the distance between the equilibrium value of  $u$  and upper limitation is five times as large as the distance between equilibrium  $u$  and lower limitation ( $|u_{\max} - u_{\text{eq}}| = 5|u_{\text{eq}} - u_{\min}|$ ). For almost all parameters

in the Turing space (see Fig. 2), the model generated spot patterns in which white spots of high  $u$  are evenly scattered and the black areas are connected with each other. Figure 2b shows the results when the distance between the equilibrium value of  $u$  and upper limitation is equal to the distance between the equilibrium and lower limitation ( $|u_{\max} - u_{\text{eq}}| = |u_{\text{eq}} - u_{\min}|$ ). The stripe patterns appeared in almost all area of Turing space, in spite that striped patterns are considered rather difficult to generate by reaction diffusion models (MURRAY, 1989). Figure 2c shows the results when the distance between equilibrium value of  $u$  and upper limitation is five times small as the distance between equilibrium point of  $u$  and lower limitation ( $5|u_{\max} - u_{\text{eq}}| = |u_{\text{eq}} - u_{\min}|$ ). Figure 2c shows the distribution of the generated patterns at each parameter in Eqs. (1) and (4) with constraint Eq. (5). Now, the reversed spot patterns, which are very hard to produce by many nonlinear models, appeared in almost all area of Turing space.

Comparison of three cases in Fig. 2 suggests that the relative position of the equilibrium  $u$  between upper limitation and lower limitation plays a critical role in determining the pattern to form. If the difference between equilibrium  $u$  to upper limitation and that between equilibrium and lower limitation are similar, the stripe patterns will emerge. If the difference between equilibrium  $u$  and upper limitation is larger than the difference between the equilibrium and lower limitation, spot patterns will emerge. In contrast, the difference between equilibrium  $u$  and lower limitation is larger than that to upper limitation, the reversed spot patterns will emerge. The result is independent of the absolute size of the constrain interval, but only depends on the relative position of the equilibrium between upper and lower limitations. We also examined the effect of  $d$ , the magnitude of diffusion coefficient of inhibitor relative to that of the activator. The size of the Turing space changed with  $d$ , but the patterns generated by the model in the Turing space was independent of  $d$ . See SHOJI *et al.* (2003b) for details.

### 3.3. Pattern selection of nonlinear reaction terms

To relate the conclusion of the constrained linear kinetics with the behavior of general nonlinear models, we noted the shape of null-clines of the ordinary differential equations. Lower and upper limitations of activator level  $u$  to be Eq. (5) can be realized by an additional term in the right hand side of Eq. (1) which are very small within the interval but becomes very large near the points of limitation. For example a lower limitation " $u \geq u_{\min}$ " can be realized by a factor that is very small in magnitude for  $u > u_{\min}$ , but becomes a positive term with a very large magnitude near  $u \approx u_{\min}$ . An upper limitation of  $u \leq u_{\max}$  can be realized by a term that is very small in magnitude for  $u < u_{\max}$  but becomes clearly negative with a large magnitude near  $u \approx u_{\max}$ . We can produce such a constraint by additional terms,  $(u_{\min}/u)^{10} - (u/u_{\max})^{10}$ , in  $du/dt$  in Eq. (4). Figure 3 illustrates the null-clines of the linear reaction term (Fig. 3a), and linear terms with additional constrain terms as discussed above (Fig. 3b).

If we draw null-cline for  $u, f(u, v) = 0$  for the model with additional terms for constraint, it has a sharp increase near the lower limitation ( $u \approx u_{\min}$ ) and a sharp decline near the upper limitation ( $u \approx u_{\max}$ ). This is illustrated clearly by the contrast between Fig. 3b (with constraint) and Fig. 3a (without constraint). Hence the constraint modifies the shape of null-cline  $f(u, v) = 0$ . Conversely, if a null-cline of a given non-linear model increases sharply at a low level or if the null-cline decreases sharply at a high level, we can guess that

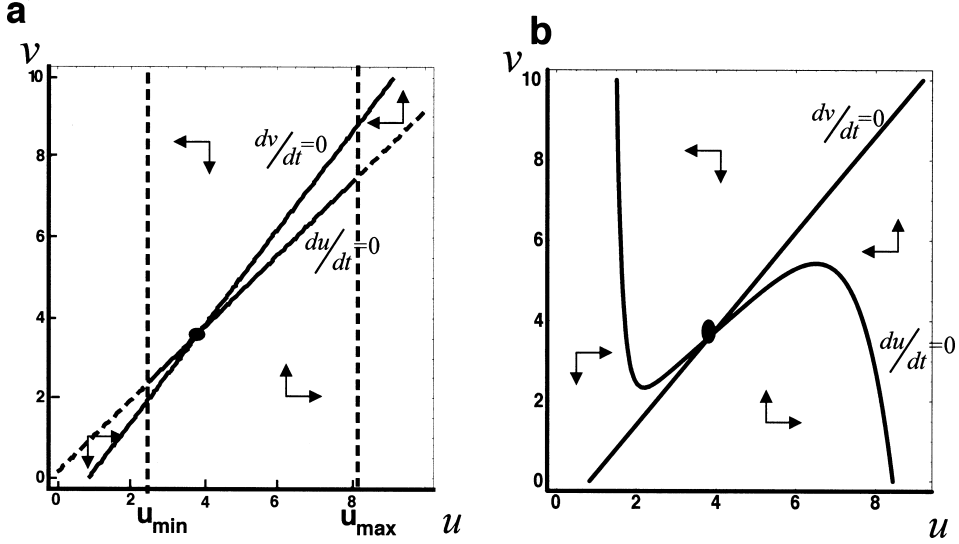


Fig. 3. The null-clines. (a) Linear kinetics given by Eq. (4). (b) The null clines of a modified model with linear reaction terms of Eq. (4) with additional constraint terms,  $(u_{\min}/u)^{10} - (u/u_{\max})^{10}$ .

the reaction terms in fact have a property working effectively as the lower and upper limitations.

The nonlinear dynamics proposed previously for Turing mechanisms may have null-clines similar to the ones with linear dynamics with additional terms for constraint. We may discuss their similarity and difference by examining their null-clines:  $f(u, v) = 0$  and  $g(u, v) = 0$ . Combining this with the result of linear kinetics with constraint—the relative location of equilibrium to the lower or to the upper limit of the model can make spot, stripe or reversed stripe. In SHOJI *et al.* (2003b), we examined the shape of null-clines of nonlinear Turing models and discussed insights obtained on their behavior of pattern selection from the result of linear kinetics and constraint.

### 3.4. Frequency distribution of activator level

The effect of constraints to the spatial patterns generated by the model can be understood more intuitively by examining the distribution of activator level.

The distribution of sampled values of activator level  $u$  for a stripe pattern are of M-shape with two peaks in the highest and the lowest value and with rather low level in the intermediate value. In contrast, the distribution of sampled  $u$  value for a spot pattern is shifted toward left and a tail toward right. In contrast, the distribution of  $u$  for a reversed spot pattern has a peak toward right. We generated the distribution of activator level  $u$  for spatial patterns generated by linear and nonlinear models with or without additional constraints, with many different parameter values. However we always have a clear correspondence of the spatial pattern (spot, stripe, or reversed stripe) and the shape of distributions (see SHOJI *et al.* (2003b) for detail).

We can quantify the difference between these by a third moment of the distribution of activator level  $u$ . According to the simulations with different reaction terms and different parameters, the average of  $u$  is almost always very close to the equilibrium value. When the distribution are lean to leftward, the third moment is positive, and when the distribution are lean to rightward, it is negative. We can clearly classify the patterns by using the third moment. When the third moment is clearly positive, the patterns are of spot patterns. When the third moment are nearly equal 0, the patterns are stripe patterns. When the third moment are clearly negative, the patterns are reversed spot patterns. This result holds for different choice of reaction terms and parameters.

Based on this result, the effect of constraints from above or from below can be understood intuitively. A two-dimensional Turing pattern determines the relative position of the equilibrium point between upper and lower limitations. If the limitation from below is closer to the equilibrium than the limitation from the above, and if the mean is close to the equilibrium value, this would produce a positive third moment of the distribution of  $u$ . Hence this explains why spot patterns are generated (white spots are scattered over black region). In contrast if the limitation from above is closer to the equilibrium than that from the below, a negative third moment of the distribution of  $u$  is created, resulting in reversed spot patterns (with black spots scattered over white regions). If the distance between the limitation from above to the equilibrium and that between the limitation from below to the equilibrium is similar in magnitude, we have a distribution of activator level  $u$  with the third moment close to zero, resulting in patterns with stripes.

DILLON *et al.* (1994) analyzed pattern formation of Turing system with several different boundary conditions (i.e. Neumann boundary condition, Dirichlet boundary condition, and the boundary condition of the mixture of these two) for one-dimensional model. MURRAY (1989) also studied the effect of boundary conditions mathematically for two-dimensional models.

#### 4. Directionality of Stripes in the Fish Skin

In this section, we focus on the directionality of stripes. Most of the stripes observed on fish skins are either parallel or perpendicular to their anterior-posterior (AP) axis, and the direction of the stripes is characteristic to each developmental stage and each species, although the pattern may change as the fish grows. For example, closely related pair of species in this genus (*Genicanthus melanosphilos* and *Genicanthus watanabei*) show different stripe patterns: *G. melanosphilos* has stripes perpendicular to AP axis and *G. watanabei* has stripes parallel to the anterior-posterior axis (see figure 1 of SHOJI *et al.*, 2003a). The direction of stripes is considered of importance in the behavioral and ecological viewpoints—in the case of African cichlid fishes, the vertical stripes tend to be associated with living in rocky substrate or vegetation, whilst the horizontal stripes are associated with schooling behavior (SEEHAUSEN *et al.*, 1999). On the other hand, we do not know the developmental mechanisms determining the directionality in fish skin.

##### 4.1. Modeling of anisotropic diffusion

In two closely related species (*Genicanthus melanospilos* and *G. watanabein*), striped pattern is absent in the female stage and stripes are formed when the fish change sex to male.

The directionality of the stripes differ between them strikingly. In both species, careful examination of this process shows that the directionality of the pattern start all over the skin, rather than started at a localized place and spread (see figure 1 of SHOJI *et al.*, 2003a). First many black spots appear at random. Then they become elongated, and then fuse with each other and final form the stripes (SHOJI *et al.*, 2003a). This suggests that the directionality of the pattern is created by the anisotropy of skin, rather than forced by the shape of boundary of the region. We conjecture that the scales are responsible for the directionality. Most fish with directional stripes have body covered by the skin with scales arranged orderly. On the other hand, the stripes of scale-less fish, e.g. popper fish, often do not have clearly directional skin patterns. Even in the fish with directional stripes, scale-less region of the skin has non-directional patterns, exemplified by Napoleon fish (see figure 2a of SHOJI *et al.*, 2003a).

If we see the cross-section of the fish skin along the AP axis, melanophores which are located beneath the skin epithelia where scales are present. Scales of *Genicanthus* are symmetric along the dorsal-ventral (DV) axis, and the anterior region of the scales is buried in the dermis of the fish skin (see figure 2c of SHOJI *et al.*, 2003a). We believe that this conformation might cause directionality in affecting local neighbors, which is expressed as the anisotropy of diffusion in the Turing model. Then the magnitude of the anisotropy is likely to be different between the two substances.

To introduce anisotropic diffusion into Turing system, we assumed that the diffusion coefficient depends on the direction of flux of the substance:

$$\frac{\partial u}{\partial t} = \nabla \cdot (D_u(\theta_u)\nabla u) + \mathcal{F}(u, v), \quad \text{and} \quad \frac{\partial v}{\partial t} = d\nabla \cdot (D_v(\theta_v)\nabla v) + \mathcal{G}(u, v). \quad (6)$$

The diffusion coefficient of the two substances are

$$D_u(\theta_u) = \frac{1}{\sqrt{1 - \delta_u \cos(2(\theta_u - \psi_u))}}, \quad \text{and} \quad D_v(\theta_v) = \frac{1}{\sqrt{1 - \delta_v \cos(2(\theta_v - \psi_v))}}, \quad (7a)$$

where  $\theta_u$  and  $\theta_v$  indicate the angle of the gradient vectors of  $u$  and  $v$ , respectively. These are written as:

$$\theta_u = \arctan\left(\frac{\partial u}{\partial y} / \frac{\partial u}{\partial x}\right), \quad \text{and} \quad \theta_v = \arctan\left(\frac{\partial v}{\partial y} / \frac{\partial v}{\partial x}\right). \quad (7b)$$

The flux of each substance is proportional to the gradient vector, but the multiplication coefficient depends on the angle of the vector. Equation (7a) implies that the diffusivity of  $u$  is the largest for  $\theta = \psi_u$  and its opposite direction  $\theta = \psi_u + \pi$ , and that it is the smallest for directions perpendicular to these ( $\theta = \psi_u + \pi/2$  and  $\theta = \psi_u + 3\pi/2$ ). Similarly,  $\psi_v$  is the direction of the highest diffusivity for  $v$ . In the following we call  $\psi_u$  and  $\psi_v$  as the ‘‘diffusive direction’’ of  $u$  and  $v$ , respectively.  $\delta_u$  and  $\delta_v$  are the magnitude of anisotropy for  $u$  and  $v$ ,

respectively. These satisfy  $0 \leq \delta_u < 1$  and  $0 \leq \delta_v < 1$ . A case of  $\delta_u = 0$  and  $\delta_v = 0$  implies the isotropic diffusion. This form of anisotropic diffusion was adopted by KOBAYASHI (1993) in his study of dendritic crystal formation, but the functional forms of  $D_u(\theta)$  and  $D_v(\theta)$  adopted by Kobayashi were different from ours.

#### 4.2. Spatial patterns generated

We calculated the model given by Eqs. (6) and (7) numerically. We studied the case with reaction terms known as “activator-depleted substrated model” which was first proposed by GIERER and MEINHARDT (1972) and analyzed in detail by SCHNACKENBERG (1979). This model is more robust in forming striped spatial pattern than other choices of reaction terms (ERMENTROUT, 1991; LYONS and HARRISON, 1992). The reaction terms are

$$f(u, v) = A - u + u^2v, \quad \text{and} \quad g(u, v) = B - u^2v, \quad (8)$$

where  $A$  and  $B$  are positive constants. We chose parameter value as:  $A = 0.025$ ,  $B = 1.550$ ,  $d = 20.0$ ,  $\gamma = 10000$ , which make stripes patterns in Eqs. (1) and (8) (DUFIET and BOISSONADE, 1992). We also examined different parameter values and different reaction terms, but the result remained qualitatively the same as far as stripes formed in the final pattern (SHOJI *et al.*, 2002). The same simulation technique was used except for the time mesh. When both  $\delta_u$  and  $\delta_v$  are less than 0.4, time mesh size was  $10^{-6}$ . Otherwise the mesh size was  $5 \times 10^{-7}$ . These were chosen to satisfy the stability condition for numerical analysis. The results concerning the directionality of obtained stripe patterns were the same for the three initial conditions. To obtain the final spatial distribution, we ran the model for a sufficiently long time. From a given spatial distribution of  $u$ , we calculated the direction of stripes using an algorithm explained in appendix A of SHOJI *et al.* (2002).

Figure 4 shows stripe patterns generated by Eqs. (6)–(8) when  $\psi_u = \psi_v = 0$ . The anisotropic diffusion of  $u$  and isotropic diffusion of  $v$  produced stripes parallel to the common diffusive direction (Fig. 4a). In contrast, the anisotropic diffusion of  $v$  and isotropic diffusion of  $u$  make stripes perpendicular to the diffusive direction (Fig. 4b).

The direction of stripes to be formed depends critically on the relative magnitude of anisotropy. When anisotropy of  $u$  is stronger than that of  $v$  ( $\delta_u \geq \delta_v$ ), stripes are formed parallel to the diffusive direction, whilst, if anisotropy of  $v$  is larger than that of  $u$  ( $\delta_u < \delta_v$ ), the stripes are formed perpendicular to the diffusive direction. Figure 5 shows the summary of the direction of stripe patterns obtained by the anisotropic diffusion model. Horizontal and vertical axes indicate  $\delta_u$  and  $\delta_v$ , respectively. Each point indicates the direction of the observed stripe: horizontal (○); vertical (●); or not-determined (×). This phase plane is separated into a domain in which stripes were parallel to the diffusive direction (horizontal stripes) and another domain in which stripes were perpendicular to the diffusive direction (vertical stripes). In between these two, there is a narrow band in which the direction of stripes could not be determined by the algorithm (e.g. in Fig. 4c), indicated by the “×” marks in Fig. 5.

Most of fish species with stripe pattern on their skin have stripes either parallel or perpendicular to their anterior-posterior axis. Very few species has stripes of random

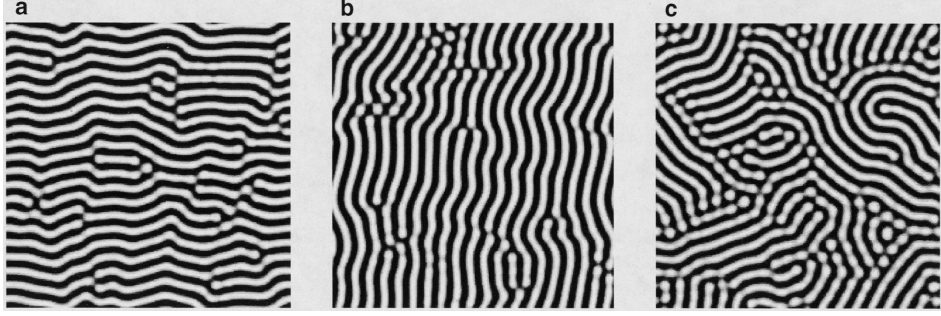


Fig. 4. The stripe patterns generated by Eqs. (6)–(8). Both substances have the fastest diffusion in the same direction:  $\psi_u = \psi_v = 0$ . Anisotropy of two substances are: (a)  $\delta_u = 0.2$ ,  $\delta_v = 0.0$ ; (b)  $\delta_u = 0.0$ ,  $\delta_v = 0.2$ ; (c)  $\delta_u = \delta_v = 0.1$ . Other parameters are fixed at:  $a = 0.025$ ,  $b = 1.550$ ,  $d = 20.0$ , and  $\gamma = 10000$ . The anisotropic diffusion of  $u$  makes stripes parallel to the diffusive direction. In contrast, the anisotropic diffusion of  $v$  makes stripes perpendicular to the diffusive direction. When the value of anisotropy are the same between  $u$  and  $v$ , the pattern has of stripes but no clear directionarity.

direction. The above result suggests that the diffusive direction to make stripes is the same between the two substances. First we described two closely related species of fish (*Genicanthus melanospilos* and *G. watanabein*), which are very similar in size, morphology and ecology except that the direction of the stripes that appear as they change sex is vertical in one species and horizontal in the other. If the anisotropy of diffusion of the two substances is responsible for the contrasting difference between these two species, a small difference in the magnitude of anisotropy can explain a very large difference in the direction of stripes on fish skin.

#### 4.3. Search for unstable modes—An heuristic approach

To know the direction of stripes to be formed by the anisotropic diffusion model (Eqs. (6) and (7)), we developed an heuristic argument (SHOJI *et al.*, 2002). Let  $(u_0, v_0)$  be the equilibrium of the ordinary differential equations given by reaction terms. We consider a small deviation from the uniform steady state  $(u, v) = (u_0, v_0)$ , as follows:

$$u = u_0 + A \cos(k_x x + k_y y) d^{\lambda t}, \quad \text{and} \quad v = v_0 + B \cos(k_x x + k_y y) d^{\lambda t}, \quad (9)$$

where  $A$  and  $B$  are small constants. Equation (9) indicates a spatial pattern with stripes having normal vector equal to  $(k_x, k_y)$ . If  $\lambda < 0$ , the mode given by Eq. (9) decreases in size. In contrast, if  $\lambda > 0$ , the mode grows exponentially with time. We replace Eq. (9) in the linearized dynamics of Eqs. (6) and (7) calculated around  $(u, v) = (u_0, v_0)$ . For any given  $(k_x, k_y)$ , we can construct a solution of the form Eq. (9) by choosing  $\lambda$  at an appropriate value. If all the solutions of form Eq. (9) have a negative  $\lambda$ , the uniform steady state is stable against these modes of deviation with stripes. If instead there are many solutions of the form given by Eq. (9) with different  $(k_x, k_y)$  and  $\lambda > 0$ , the mode with the largest positive

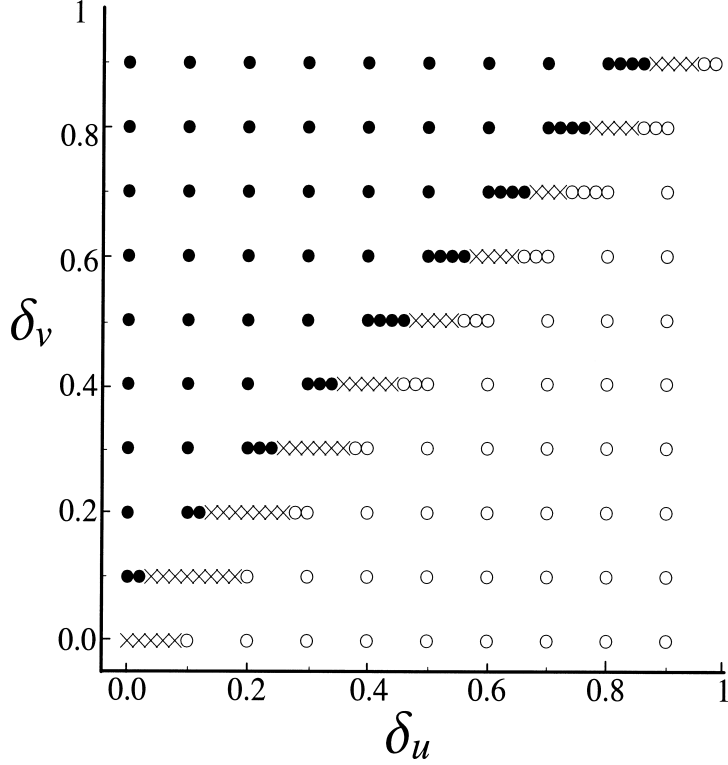


Fig. 5. Summary of the direction of stripe patterns obtained by the anisotropic diffusion model. Horizontal and vertical axes indicate  $\delta_u$  and  $\delta_v$ , respectively. Symbols indicate the direction of the observed stripe: horizontal ( $\circ$ ); vertical ( $\bullet$ ); or not-determined ( $\times$ ). In order to know whether a spatial pattern has stripes with a fixed direction and to quantify the direction in which the stripes are formed, we adopted an index based on the spatial auto-correlation (explained in SHOJI *et al.*, 2002). The spatial patterns were generated from Eqs. (6)–(8). The direction for the fastest diffusivity was the same between two substances:  $\psi_u = \psi_v = 0$ .

$\lambda$  is the one that grows at fastest rate. We may compare the direction of this most unstable stripe calculated from linear analysis with the stripe in the final spatial pattern formed by the nonlinear dynamics Eq. (8). Note that the stripes to be formed are perpendicular to vector  $(k_x, k_y)$ , because it is a normal vector.

From Eq. (9), we can derive  $\theta_u = \theta_v = \arctan(k_y/k_x)$ , which implies that the gradient vectors of both  $u$  and  $v$  take a fixed direction that is perpendicular to vector  $(k_x, k_y)$ . In appendix B of SHOJI *et al.* (2002), we search for the squared length of the vector,  $\sqrt{k_x^2 + k_y^2}$ , and the angle of the vector,  $\theta = \arctan(k_y/k_x)$ , which realize an approximately maximum positive  $\lambda$ . Then the length of the vector is related (inversely) to the distance between adjacent stripes and the angle corresponds to the (perpendicular) direction of stripes in the pattern. We can prove that the mode of deviation  $(k_x, k_y)$  that achieves an approximately

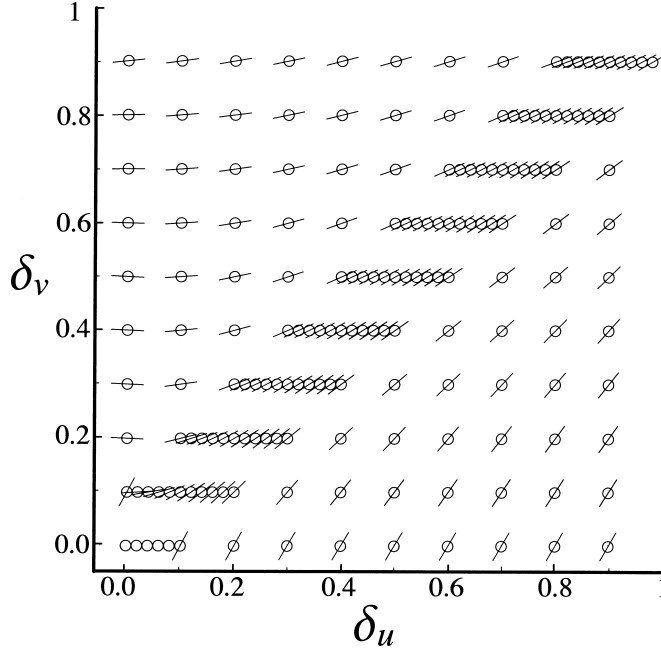


Fig. 6. The diagram illustrating the directionality of stripes. A short line passing through an open circle indicates the direction parallel to the stripes formed in the final spatial pattern when anisotropy of the two substances are given by the location of the circle  $(\delta_u, \delta_v)$ . The direction of stripes is calculated by the algorithm in SHOJI *et al.* (2002). The spatial patterns were generated from Eqs. (6)–(8). The direction for the fastest diffusivity was different between two substances:  $\psi_u = \pi/3$  and  $\psi_v = \pi/2$ .

maximum  $\lambda$  has angle  $\theta = \arctan(k_y/k_x)$  that maximizes the following quantity:

$$\eta(\theta) = \frac{D_v(\theta)}{D_u(\theta)} = \sqrt{\frac{1 - \delta_u \cos(2(\theta - \psi_u))}{1 - \delta_v \cos(2(\theta - \psi_v))}}. \quad (10)$$

See appendix B of SHOJI *et al.* (2002) for the argument leading to this result. In the following we examine the angle that maximizes Eq. (10), denoted by  $\theta_{\text{predicted}}$ .

When we consider first the case in which the diffusive direction of two substances is the same (i.e.  $\psi_u = \psi_v$ ), we should examine the maximum of  $\eta^2 = (1 - \delta_u w)/(1 - \delta_v w)$ , when  $-1 \leq w \leq 1$ , by setting  $w = \cos(2(\theta - \psi))$ . By drawing the graph of this function, we can conclude as following:

If  $\delta_u > \delta_v$ , stripes are formed parallel to the diffusive direction.

If  $\delta_u < \delta_v$ , stripes are formed perpendicular to the diffusive direction.

If  $\delta_u = \delta_v$ , there is no specific direction for stripes.

This is consistent with the simulation results (SHOJI *et al.*, 2002).

#### 4.4. When the diffusive directions differ: $\psi_u \neq \psi_v$

In the last section, both substances are assumed to have the highest diffusivity in the same direction. We may also consider the general case in which the direction of maximum diffusivity can be different between the two substances.

The same method predicts the direction of stripes to form. When anisotropy is small for both substances ( $\delta_u \ll 1$ , and  $\delta_v \ll 1$ ), by expanding  $\eta(\theta)^2$  with eliminating the higher order terms, SHOJI *et al.* (2002) predict that the stripe patterns to be formed should have a normal vector with the angle given by

$$\theta_{\text{predicted}} = \frac{1}{2} \arctan \left[ \frac{\delta_u \sin 2\psi_u - \delta_v \sin 2\psi_v}{\delta_u \cos 2\psi_u - \delta_v \cos 2\psi_v} \right] + \frac{\pi}{2}. \quad (11)$$

When the most diffusive direction is different (not parallel) between the two substances, the direction of stripes changes smoothly from the diffusive direction of  $u$  to the direction perpendicular to the diffusive direction of  $v$  as the anisotropy of  $u$  and  $v$  change smoothly. Figure 6 illustrates the direction of the stripes in the final spatial pattern when  $\psi_u = \pi/3$  and  $\psi_v = \pi/2$ . The predicted direction is very close to the direction of the stripes observed in simulation results (see figure 5 of SHOJI *et al.*, 2002, in which we compared the predicted directions with obtained one in case  $\psi_u = \pi/3$  and  $\psi_v = \pi/6$ ).

## 5. Discussion

In this paper, we have reviewed a series of papers on two-dimensional pattern formation of Turing systems that are motivated by pattern formation of fish skin (SHOJI *et al.*, 2002, 2003a, 2003b).

First, we discussed the effect of the choice of reaction terms on pattern selection. We examined the model with linear reaction terms and additional constraint terms which confine the variables within a finite range. We first show that in a one-dimensional model, a periodic stationary pattern can be formed only when activator level is constrained both from below and from above. The constraint of inhibitor is irrelevant. In the two-dimensional model, the relative distance of the equilibrium level of activator between the upper and lower limitations determines the pattern selection. Patterns with stripes are produced when the equilibrium is equally distant from the upper and the lower limitations, but patterns with spots are produced when the equilibrium is clearly closer to one than to the other of two limitations. We then attempt to explain the pattern selection of nonlinear models based on the result of linear models with constraints. The distribution of activator level is skewed positively and negatively for spot patterns and reversed spot patterns, respectively. In contrast, the skewness of the distribution of activator level was small for striped patterns. This gives an intuitive explanation of why the location of the equilibrium between constraints. We then interpreted the pattern selection of nonlinear Turing model, based on the insights obtained from the result of Turing model with linear reaction and constraints.

Second, we introduced anisotropic diffusion into diffusion term to explain the skin pattern of two closely related species of fish (*Genicanthus melanospilos* and *G. watanabein*), which are very similar in size, morphology and ecology except that the direction of the

stripes that appear as they change sex is vertical in one species and horizontal in the other. If the anisotropy of diffusion of the two substances is responsible for the contrasting difference between these two species, a small difference in the magnitude of anisotropy can explain a very large difference in the direction of stripes on fish skin. According to the discussion in this review, such a discontinuous change in the direction of stripes can be observed only when the direction of anisotropy of the two substances coincides. If the diffusive directions of the two substances are different, we should observe a continuous change in the directionality of stripes caused by smooth change in parameters. Considering the strong similarity of the two species in genus *Genicanthus*, the theoretical study suggests that anisotropy of the two substances expressed in reaction-diffusion model is responsible for determining the direction of stripes and that the diffusive direction of the two substances must be the same.

Turing models give the basic logic in biological pattern formation. They have been studied mathematically over half a century since the seminal paper was proposed (TURING, 1952). However in most of these studies, the model stays phenomenological because of our lack of knowledge on the underlying processes of morphogenesis. However the situation is going to change very soon. Thanks to quick development of molecular biology in the later half of the last century, we are going to get detailed molecular basic of pattern formation and development of organisms. This will give us a great opportunity to develop mathematical and computational models that consider those newly available information and that are fully based on the knowledge of mechanistic basis. We predict that Turing models would still give the basis of the biological pattern formation, and the importance of the Turing idea will become even more clearer as the result of the progress of mathematical study of biological pattern formation.

This work was supported in part by a Grant-in-Aid from the Japan Society for the Promotion of Science to Y.I. We are grateful for Professor Shigeru Kondo, Center for Developmental Biology, RIKEN Kobe and Dr. Atsushi Mochizuki, National Institute for Basic Biology, for their help. We also thank the following people for their helpful comments: R. Kobayashi, M. Mimura, T. Ohta, A. Sasaki, and S. Tohya.

#### REFERENCES

- ASAI, R., TAGUCHI, R., KUME, Y., SAITO, M. and KONDO, S. (1999) Zebrafish Leopard gene as a component of putative reaction-diffusion system, *Mech. Dev.*, **89**, 87–92.
- DILLON, R., MAINI, P. K. and OTHMER, H. G. (1994) Pattern formation in generalized Turing systems I. Steady-state patterns in systems with mixed boundary conditions, *J. Math. Biol.*, **32**, 345–393.
- DUFLET, V. and BOISSONADE, J. (1992) Conventional and unconventional Turing pattern, *J. Chem Phys.*, **96**, 664–673.
- ERMENTROUT, B. (1991) Stripes or spots? Nonlinear effects in bifurcation of reaction-diffusion equations on the square, *Proc. R. Soc. Lond.*, **A434**, 413–417.
- GIERER, A. and MEINHARDT, H. (1972) A theory of biological pattern formation, *Kybernetik*, **12**, 30–39.
- KOBAYASHI, R. (1993) Modelling and numerical simulations of dendritic crystal growth, *PhysicaD*, **63**, 410–423.
- KONDO, S. and ASAI, R. (1995) A reaction-diffusion wave on the marine angelfish *Pomacanthus*, *Nature*, **376**, 765–768.
- KUWAMURA, T. and KARINO, K. (1999) Mimicry of fishes, in *Mimicry* (ed. K. Ueda), pp. 1–15, Tsukiji shokan, Tokyo (in Japanese).

- LYONS, M. J. and HARRISON, L. G. (1992) Stripe selection: An Intrinsic property of some Pattern-Forming models with nonlinear dynamics, *Devel. Dyn.*, **195**, 201–215.
- MEINHARDT, H. (1982) *Models of Biological Pattern Formation*, Academic Press, London.
- MURRAY, J. D. (1989) *Mathematical Biology*, 2nd ed., Springer, New York.
- SCHNACKENBERG, J. (1979) Simple chemical reaction systems with limit cycle behavior, *J. Theor. Biol.*, **81**, 389–400.
- SEEHAUSEN, O., MAYHEW, P. J. and VAN ALPHEN, J. J. M. (1999) Evolution of color patterns in East African cichlid fish, *J. Evol. Biol.*, **12**, 514–534.
- SHOJI, H., IWASA, Y., MOCHIZUKI, A. and KONDO, S. (2002) The directionality of stripes formed by anisotropic reaction-diffusion model, *J. Theor. Biol.*, **214**, 549–561.
- SHOJI, H., MOCHIZUKI, A., IWASA, Y., HIRATA, M., WATANABE, T., HIOKI, S. and KONDO, S. (2003a) Origin of directionality in fish stripe pattern, *Devel. Dyn.*, **226**, 627–633.
- SHOJI, H., IWASA, Y. and KONDO, S. (2003b) Stripes, spots, or reversed spots in two-dimensional Turing system, *J. Theor. Biol.* (in press).
- TURING, A. M. (1952) The chemical basis of morphogenesis, *Phil. Trans. R. Soc. Lond.*, **B237**, 37–72.
- YAMAGUCHI, M. (2002) *Aqua Life*, Marine Planning International, Tokyo (in Japanese).